Stimuli-Responsive Materials with Self-Healing Antifouling Surface via 3D Polymer Grafting

*Hidenori Kuroki, Ihor Tokarev, Dmytro Nykypanchuk, Ekaterina Zhulina, and Sergiy Minko**

A novel stimuli-responsive material is reported with the self-healing antifouling surface via 3D polymer grafting. The self-healing surface is generated from a polymer network and polymeric chains grafted both to the surface of the network and inside the host network material. In the conventional approach to an antifouling surface via grafting of polymer brushes, the degradation and detachment of grafted polymeric chains would expose the underlying layer, leading to a loss of the antifouling effect. If a substantial fraction of the grafted polymers is degraded and detached, the proposed material with 3D polymer grafting retains its antifouling property due to the spontaneous (driven by an emerging gradient in a chemical potential) replacement of detached or damaged polymeric chains with segments of the chains stored inside the film in proximity to the interface. The pH-responsive poly(2-vinylpyridine) films with the 3D grafting of poly(ethylene oxide) in physiological conditions (pH 7.4 and 37 °C) demonstrate a 4-fold increase in longevity of antifouling behavior than the material with the surface grafted polymer. At the same time, the 3D grafted responsive films retain their pH-responsive properties. The proposed 3D polymer-grafting can be carried out on various surfaces (polymers, nanofiber mats, nanoporous inorganic materials, etc.) and, hence, can aid in the design of advanced biointerfaces for biomedical and biotechnological applications.

1. Introduction

Living organisms demonstrate diverse stimuli-responsive behavior that is vital for their life and interactions with the host environment. One such response is self-healing. Capabilities to synthesize, regenerate and replace tissues in living systems are demanded for man-made materials for different applications. Among them is the capability to maintain long-lasting antifouling properties using self-healing behavior preprogrammed in the material.

Variations in the surrounding environment (pH, ionic strength, temperature, chemical reagents, etc.) of nanostructured stimuli-responsive polymeric materials (e.g., polymer brushes, polymer gels, nanogels, thin films, etc.) cause both chemical (ionization, formation or breaking of chemical bonds, isomerization, etc.) and physical (mechanical, optical, electroconductive, etc.) property changes within the materials. These tunable physical properties are used for the triggered release of drugs, changes in the shape and mechanical properties of artificial implants, plasmon coupling in biosensors, regulation of the permeability of bioseparation membranes and cell adhesion, and so on.[1] Quite often the changes in chemical and physical properties are in conflict with the complex environment of the materials. For example, stimuli-triggered changes of initially inert drug delivery capsules, contrast agents or shape memory implants may transform these biomaterials into objects that are targeted by the immune system due to the changes in the hydrophobic behavior, electrical charge or functional groups that frequently accompany the stimuli-responsive behavior of the materials. This problem is solved using a decoration of the material's surface with a grafted inert hydrogel coating (tethered polymer brushes or networks).[2,3] The hydrogel coating prevents short-range nonspecific interactions and long-range electrostatic interactions provided that the coating is about or greater than a few nanometers in thickness (note that under physiological conditions the Debye screening length is about 1 nm). Such antifouling coatings have numerous industrial and biotechnological applications.[4] However, an aging and loss of the antifouling properties are limitations in many applications.

Here, we propose a novel coating with a 3D grafted polymer structure for rendering a surface with long-lasting antifouling properties as illustrated in **Figure 1**. Figure 1a shows the conventional approach to an antifouling surface by the grafting

Dr. H. Kuroki, Dr. I. Tokarev, Prof. S. Minko
Department of Biomolecular Science
Clarkson University
Potsdam, NY 13699 USA
E-mail: sminko@clarkson.edu
Dr. D. Nykypanchuk
Brookhaven National Laboratory
Center for Functional Nanomaterials
Upton, NY 11973–5000, USA
Dr. E. Zhulina
Institute of Macromolecular Compounds
Russian Academy of Sciences
St. Petersburg 199004, Russia

DOI: 10.1002/adfm.201300363

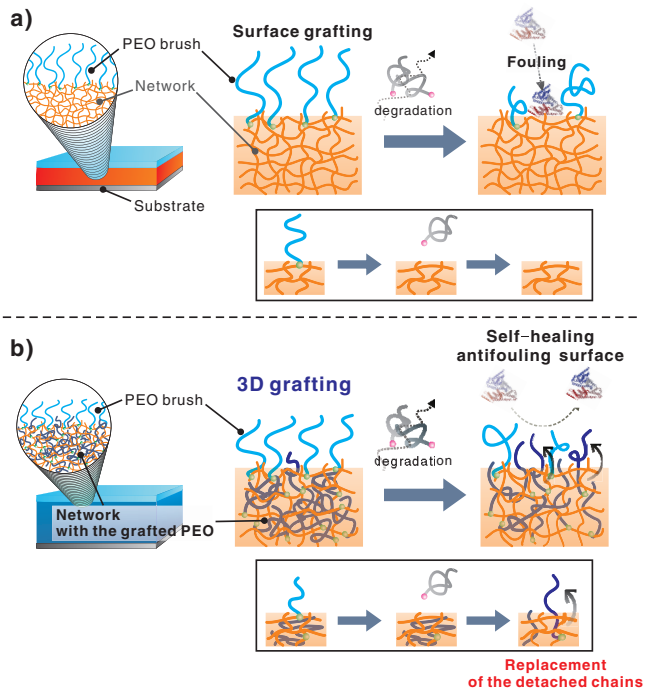

Figure 1. Schematic illustration of the PEO-grafted P2VP network films: a) the grafting of PEO to the surface of a P2VP film and b) 3D polymer grafting on the surface and inside of a P2VP film. The self-healing aspect of the antifouling property is due to the rearrangement of internally grafted polymers to the interface (marked as dark blue chains).

of polymer brushes. In this approach, degradation and detachment of the grafted polymeric chains would expose the underlying layer, leading to a loss of the antifouling effect. The proposed coating with the 3D grafting (Figure 1b), which consists of polymeric chains grafted both to the surface and inside the polymeric host material, has the potential to retain the antifouling effect, even if a substantial fraction of the grafted polymers is degraded and detached. The self-healing mechanism of the proposed structure refers to the replacement of the detached or damaged polymeric chains by segments of the chains stored inside the film in proximity to the interface. A number of segments of the stored grafted chains relocate from the film's interior driven by an emerging gradient in a chemical potential, and an antifouling effect in the exposed area can thus be recovered by itself.

The proposed concept is experimentally proven for poly(ethylene oxide) (PEO) coatings that undergo the oxidative degradation and hydrolytic dissociation of the ester bonds used to tether the polymer. This polymer was specially selected to accelerate the experiments on the coating degradation for the study of the material's aging. We believe that the obtained self-healing effect can be extended and find practical applications in a combination with more stable hydrophilic polymers.

Many recent studies have focused on the interactions at the interface between synthetic materials and biological components on multiple scales from nucleic acids and proteins to cells and organs.[5] Self-assembled monolayers (SAMs)[6–15] and grafted polymers[16] such as polyethylene glycol (PEG) and its derivatives,[17–31] hydroxyethyl methacrylate,[32,33] carbohydrate derivatives,[34–36] zwitterionic polymers,[37–40] poly(2-methyl-2-oxazoline),[41] and polypeptoids,[42,43] to name a few, have been extensively developed to achieve high resistance to protein and cell adsorption.

A number of studies have revealed that antifouling surfaces do not possess long-term stability due to the degradation and detachment of SAMs and grafted polymer chains. The stability of grafted surfaces decorated with PEG and its derivatives in particular has been rigorously studied.[9,27–31] For example, the oligoethyleneglycol-terminated SAMs lose their cell-repellent property after seven days in serum-containing media.[9] The grafted PEG brushes began to exhibit cell adhesion after two weeks in a phosphate buffer.[27] The high-density poly(PEG methylacrylate) brushes prepared by surface-initiated polymerization were detached from the substrates within one to two days in cell culture media.[30] Common strategies for enhancing the coating's stability include producing a more stable SAMs and polymer brushes binding with the substrate, using polymers with a more stable chemical structure, and using polymer networks.[44] The latter approach is very efficient for the long-term stability of antifouling properties since the loss of the antifouling behavior will require multiple cleavage of the chemical bonds in the polymer network, in contrast to the so-called "catastrophic effect" of a single bond breakage for tethered polymers and SAMs. However, the polymer network film could not always be used for the decoration of stimuli-responsive materials (which could also be made of a stimuli-responsive polymer network) since the mechanical properties of both the stimuli-responsive material and the network coating could be in conflict on the scale of nanomaterials when the material dimensions and coating are comparable. For example, the release of a drug stored in a thermoresponsive nanogel could be inhibited by a swollen network coating since the free energy change due to the local temperature change in the nanogel particle might be not sufficient to power an additional deformation of the external antifouling network.

Combinations of networks with polymers grafted inside them have been reported in previous studies and referred to as a comb-type gel. The comb-type responsive hydrogel with freely moving chains grafted to the network exhibited a rapid response to environmental stimuli.[45–47] These materials were explored as potential carriers for the delivery of drugs and nucleic acids.[48–51] In addition, a grafted polymer capable of forming self-assembled structures inside the polymeric film can improve its physical and mechanical properties.[52] To date, the combination of a network film and 3D polymer-grafting has never been applied to creating a long-lasting antifouling surface. In this study, we report on the first demonstration of retaining low interfacial energy properties for an extended time period due to a spontaneous rearrangement of the grafted polymers residing in a polymer network film. The proposed system can aid in the design of biointerfaces for biomedical and biotechnological applications, such as biosensors, systems for the delivery of drugs and genes, scaffolds for cell cultures, implants, diagnostic devices, and membrane separation filters.

2. Results and Discussion

pH-responsive cross-linked poly(2-vinyl pyridine) (P2VP) films (10–20 nm in thickness) on the surface of Si-wafers were prepared as described elsewhere.[53,54] P2VP was crosslinked by the quaternization reaction using diiodobutane. The crosslinking density was proportional to the quaternization degree, which was defined as a number fraction of the reacted pyridine groups and varied in the 1–21% range. Afterward, PEO was grafted to the surface and inside the P2VP films. To this end, a halogen-terminated PEO was spin-coated on the P2VP films and the reaction of terminal alkyl-halogen groups with P2VP pyridine rings was conducted by annealing at 120 °C for 20 h in a vacuum; the grafting temperature was higher than the glass transition temperature of P2VP and the melting temperature of PEO, providing the proper conditions for the mobility of polymer segments. PEO chains penetrated into the P2VP network due to good compatibility of the two polymers, leading to 3D grafting of PEO. Three samples of halogen-terminated PEO were used: chloro-terminated PEO (M_n = 5.0 kg/mol [PEO-Cl-5k]), and two bromo-terminated PEOs (M_n = 5.0 kg/mol [PEO-Br-5k], and M_n = 12.3 kg/mol [PEO-Br-12k]). The terminal functional groups of PEO-Br polymers include a hydrolytically degradable ester group to produce a fast detachment of grafted polymers for long-term stability tests. The prepared PEO-grafted P2VP films were characterized by ellipsometry (Multiskop null-ellipsometer, Optrel), X-ray reflectivity (Ultima III multi-purpose diffractometer, Rigaku), water contact angle, and atomic force microscopy (AFM, Dimension 3100 Scanning Probe Microscope, Veeco Instruments) measurements (see the Experimental section for more details)

The relationship between the quaternization degree of the P2VP films and the amount of the grafted PEO is shown in **Figure 2**. It is worth noting that, the PEO grafting is strongly dependent on the quaternization degree (crosslinking degree) of the P2VP films and the molecular weight of PEO. In the case of the grafting of the lower molecular weight PEO polymers (PEO-Br-5k and PEO-Cl-5k), the grafted amount decreases as the quaternization degree increases. PEO-Br-12k plateaus at roughly 10 mg/m^2 when the quaternization degree is greater than 5%.

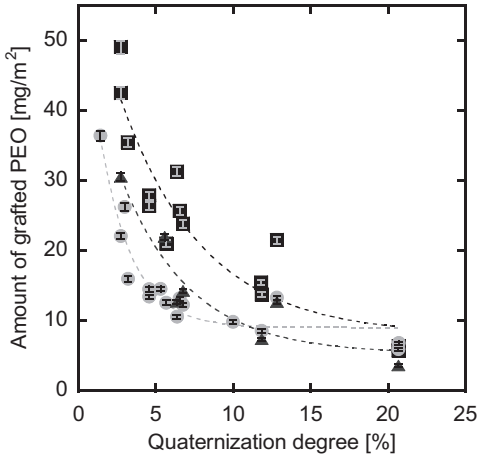

Figure 2. Amount of the grafted PEO to P2VP films with different degrees of quaternization (crosslinking) for different samples of PEO: PEO-Br-12k (●), PEO-Br-5k (■), and PEO-Cl-5k (▲).

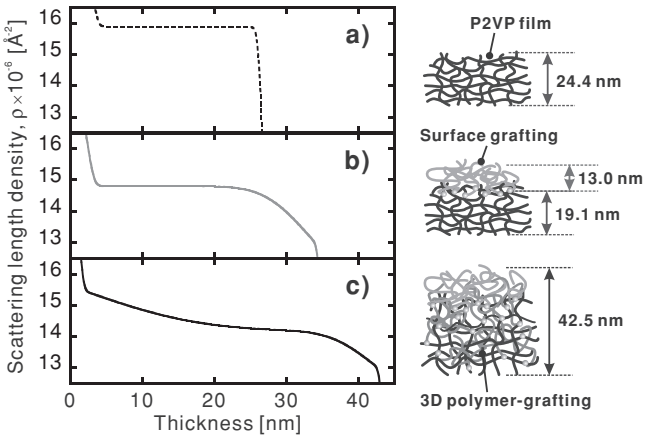

Figure 3. Scattering length density (SLD) profile of the PEO-grafted P2VP films (quaternization degree 5.7%) using X-ray reflectivity measurements in air and schematics for the film structure: a) non-grafted film, b) PEO-Br-12k, and c) PEO-Br-5k.

The composition profiles of the films were analyzed using X-ray reflectivity measurements (**Figure 3**). The quaternization degree for all the samples was 5.7%. Before the measurements, tetrachloroauric ions were bound to P2VP to contrast the P2VP layers. The reference P2VP film (Figure 3a) appears as a single layer with a constant value of scattering length density (SLD). The SLD profile of the grafted film with PEO-Br-12k chains (Figure 3b) has two distinct layers: the first one is a 19-nm thick layer with a constant density, and the second one is a 13-nm thick layer with a gradual slope. The first and second layers originate from P2VP and PEO, respectively. The gradual slope in the second layer results from the grafting of PEO chains mixed with the P2VP network at the interface. The estimated amounts and thicknesses for each layer are shown in **Table 1**.

The data obtained using ellipsometry and X-ray reflectivity are in accordance with each other (Table 1) and provide evidence that the PEO-Br-12k is grafted to the surface of the P2VP film. In contrast, the SLD profile of the film with the PEO-Br-5k is quite different from that with the PEO-Br-12k. A single layer with a gradual slope in SLD is seen in Figure 3c. The grafted film with the PEO-Br-5k is composed of the P2VP layer mixed with PEO. In other words, the PEO-Br-5k was 3D-grafted to the surface and inside the P2VP network. Thus, a large amount of PEO chains are immobilized inside the network of the 3D-grafted film; they are explored to produce an antifouling effect via their exposure to the interface, as discussed below.

The results of the grafting experiments (Figure 2) demonstrate a clear difference in the grafting behavior of the PEO-Br-5k and PEO-Br-12k polymer samples. The difference can be attributed to changes in the miscibility and diffusivity of PEO chains in the P2VP network. At a low crosslinking density (<5% quaternization degree), the PEO chains with both molecular weights of 5 kg/mol and 12 kg/mol penetrate into the P2VP network, resulting in 3D-grafting.

Table 1. The thickness and grafted amount (±0.5 nm and 0.5 mg/m^2) for each layer in the non-grafted film and PEO-grafted films.

Sample	Ellipsometry						X-ray reflectivity					
	Grafted PEO on surface		Grafted PEO inside		P2VP network	Total	Grafted PEO on surface		Grafted PEO inside		P2VP network	Total
	[mg/m^2]	[nm]	[mg/m^2]	[nm][a)]	[nm]	[nm]	[mg/m^2]	[nm]	[mg/m^2]	[nm][a)]	[nm]	[nm]
Non-grafted	0	0	0	0	23.7	23.7	0	0	0	0	24.4	24.4
PEO-Br-5k	9.7[b)]	8.9[b)]	11.3[b)]	10.4[b)]	21.5	40.8	9.7[b)]	8.9[b)]	13.2[b)]	12.1[b)]	21.5[c)]	42.5
PEO-Br12k	12.5	11.5	0	0	20.3	31.8	14.2	13.0	0	0	19.1	32.1

[a)]Change in the film thickness due to the PEO grafting inside the film; [b)]Estimations made using the data in Ref. [24]; see Supporting Information; [c)]Ellipsometry measurements.

An increase in the crosslinking (quaternization) degree results in a smaller network mesh size and, hence, a decreased mobility for the PEO chains in the network. Therefore, penetration of the PEO-Br-12k chains into the dense P2VP network is largely hindered and the polymer is surface grafted.

Besides the limited diffusivity of PEO chains, a decline in the grafted amount of the PEO-Br-5k and PEO-Cl-5k as a quaternization degree becomes higher arises from a decrease in the polymers' compatibility. The difference in the grafted amounts for the PEO-Br-5k and PEO-Cl-5k at the same degree of P2VP quaternization is due to a different reactivity of the halogen end-functional groups. Thus, a proper adjusting of the molecular mass of the grafted PEO and the quaternization degree of the P2VP network film can be explored for the synthesis of PEO-grafted P2VP network films with the controlled location of the grafted chains, as shown in Figure 1.

The topography AFM images of the PEO-functionalized P2VP films in air reveal crystallization of the surface-grafted PEO (**Figure 4**b) in accordance with earlier reports on the crystallization of PEO brushes on Si-substrates,[55] while the development of the 3D-grafting regime results in less ordered mixed structures (Figure 4c,d). The water contact angle for all the grafted films was found to be roughly 30° in contrast to roughly 70° for the P2VP crosslinked film itself.

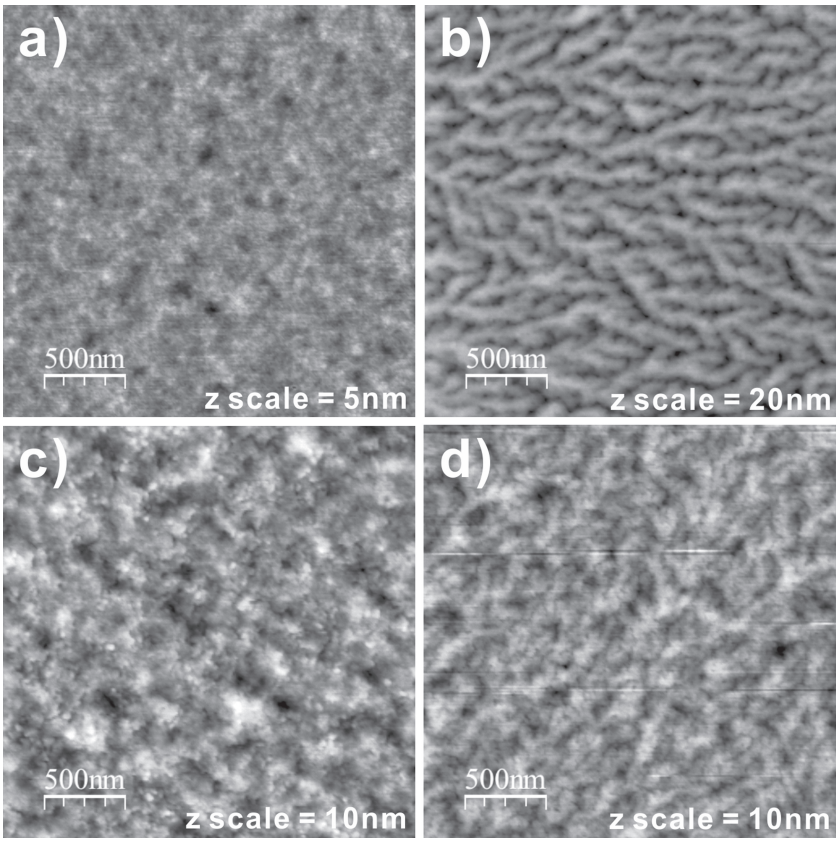

Figure 4. AFM topography images of the PEO-grafted P2VP films with the quaternization degree of 5%: a) non-grafted film, b) PEO-Br-12k, c) PEO-Br-5k, and d) PEO-Cl-5k.

Antifouling properties of the PEO-grafted films were studied by protein adsorption tests using bovine serum albumin (BSA, 67 kDa, pI 4.7) and fibrinogen (340 kDa, pI 5.5) in a phosphate buffer solution (pH 7.4). The adsorbed protein amounts were analyzed using ellipsometry measurements. It was found that the adsorbed amounts on the non-grafted P2VP films were 4.2 ng/mm^2 for BSA and 9.9 ng/mm^2 for fibrinogen, whereas the adsorbed amounts on the PEO-grafted films were negligibly small.

The aging of the samples and the stability of the antifouling property were studied in phosphate buffer solutions (pH 7.4) at 37 °C. Three different kinds of PEO-grafted films with an approximately 5% quaternization degree were used for the tests: the film with the 12.7 mg/m^2 surface-grafted PEO-Br-12k (35° water contact angle) and two 3D-grafted films with 23.9 mg/m^2 of PEO-Br-5k (32° water contact angle) and 14.2 mg/m^2 of PEO-Cl-5k (31° water contact angle). Note that the PEO-Br-5K grafting yielded the largest amount due to a combination of the surface and 3D grafting, while the PEO-Br-12k was grafted mainly to the surface, as discussed above.

Figure 5a shows changes in the amount of the grafted PEO as a function of an incubation time in the buffer solutions. The grafted amount of the films prepared using bromo-terminated PEO decreased, as expected, much faster than the film grafted

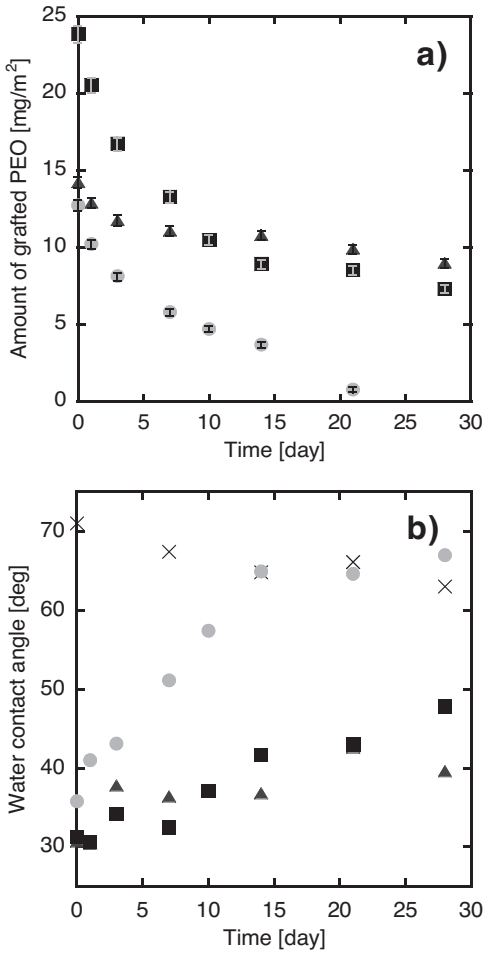

Figure 5. Stability tests for the PEO-grafted P2VP films: a) the amount of the grafted PEO, and b) the water contact angle as a function of incubation in a pH 7.4 phosphate buffer at 37 °C: non-grafted film (×), PEO-Br-12k (●), PEO-Br-5k (■), and PEO-Cl-5k (▲).

with the chloro-terminated PEO. To explain this rapid loss of grafted polymers, the stability of the free (non-grafted) PEO-Br-5k polymer in a phosphate buffer solution at 37 °C was evaluated using ^{1}H-NMR analysis. This analysis revealed that the hydrolysis reaction of the ester bond in the PEO-Br-5k end group occurred at a similar rate as the detachment of the PE-Br-5k grafted polymer (see the Supporting Information). The dominant factor for the fast decrease in the grafted amount is the hydrolysis of the ester bond in the PEO-Br-5k end groups. The PEO-Cl-5K grafted amount decreased much slower (Figure 5a) because the PEO-Cl does not include an ester bond in the end group, and thus this slow decrease could arise from an oxidative degradation of main chains in PEO, as reported elsewhere.[56,57]

It is worth noting here that, although the grafted PEO-Br-5K was quickly detached from the P2VP film, the water contact angle on the grafted film remained low for a long period of time (Figure 5b). The protein adsorption test (**Figure 6**) demonstrated the resistance of the layer to protein adsorption for at least four weeks. In contrast, the water contact angle for the PEO-Br-12k grafted film increased much faster in time, and

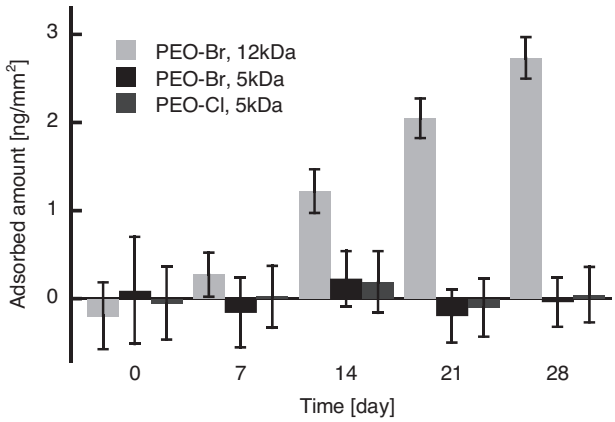

Figure 6. Adsorbed amount of fibrinogen on the grafted films as a function of incubation time in a pH 7.4 buffer solution at 37 °C, (gray) PEO-Br-12k, (black) PEO-Br- 5k, and (dark-gray) PEO-Cl-5k.

the protein adsorption was observed after just one week. Thus, the 3D-grafted structure demonstrated 4-fold higher stability under physiological conditions than the 2D surface-grafted structure.

The self-healing mechanism of the 3D-grafted films' anti-fouling property was theoretically analyzed (see Supporting Information). The volume fraction of brush monomers at the interface was calculated by the balance of the chemical potentials of grafted polymers on the surface and inside the network. For simplicity, we only considered a thin, near-surface layer of the polymer network with the grafted PEO chains, whose thickness is smaller than that of the swollen brush, thus enabling us to assume that relocating chain segments contribute with almost the same number of monomers in the brush as the chains tethered to P2VP network surface. The network-forming polymer and the grafted polymer were in similar (theta) solvent conditions. The detachment reaction was assumed to be a first-order reaction. We compared temporal changes in the concentration of PEO monomer units at the interface for two systems: system I, a surface grafted brush and system II, 3D grafting; we assumed that at time $t = 0$ both systems had the same grafting density of chains on the network surface. The results of the calculations of the monomer volume fraction on the surface in systems I and II are shown in **Figure 7**. They indicate that, in the 3D-grafting regime, a higher concentration (density) of grafted polymers is retained on the surface due to the rearrangement of polymeric chains residing in the network's interior, and that they replenish the lost PEO chains at the network interface, thus providing the basis for the self-healing effect (Figure 1). The rearrangement is driven by change in the balance of the free energy of the 3D-grafted chains in the network and 2D-brush (see Equations (2) and (3) in the Supporting Information). Since a higher polymer density increases penalty for the protein penetration into the brush,[58] the theoretical analysis implies that the 3D polymer-grafting regime will exhibit a longer-lasting antifouling effect than the surface-grafting regime (Figure 6). Obviously, the theoretically demonstrated self-healing effect will endure even longer for greater thicknesses of the PEO-grafted polymer network layer, since the network acts as a reservoir of PEO chains.

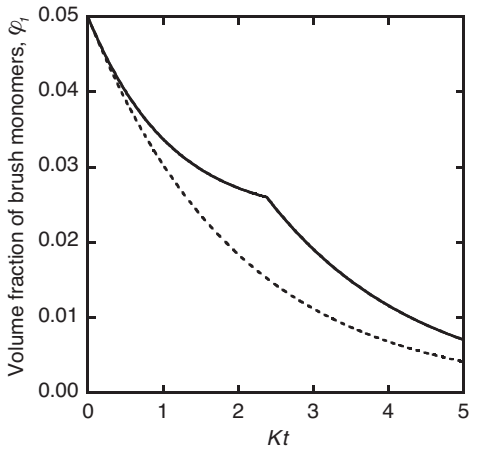

Figure 7. Changes in the volume fraction ϕ_1 of brush monomers as a function of *Kt* (dimensionless time, where *K* is the first-order hydrolysis reaction rate constant and t is the incubation time): surface grafting (dashed line), and 3D-grafting (solid line) see the Supporting Information for details.

It is worth noting that the 3D PEO-grafted P2VP film retained its pH-responsive properties (see the Supporting Information). Thus, the P2VP film, initially hostile to biological environment, turns into a protein-repellent material with long-term antifouling properties after using the novel 3D grafting approach. We intentionally selected this example of an originally non-biocompatible material and demonstrated that 3D-grafting on the surface of such a material could result in a long-lasting biocompatible interface. Many other kinds of polymer networks 3D-grafted with hydrophilic biocompatible polymers can be used for the regulation of mass transport and separation, stimuli-triggered drug release, and biosensors in biological environments.

3. Conclusions

In conclusion, a novel 3D polymer-grafting approach for a long-lasting antifouling effect has been developed in this work. We demonstrated a successful control of the location of grafted polymers in a polymer network thin film (on the surface or inside the network film) by varying the molecular weight of the grafted polymer and the crosslinking degree of the network film. The theoretical analysis showed that 3D-grafted coatings possess a long-lasting antifouling effect with a longer stability than surface grafting, while the experimental results demonstrated an example of the four-fold longer stability. This was attributed to the self-healing property rationalized by spontaneous rearrangement of the grafted PEO chains residing in the network, which results in their exposure to the interface, as depicted in Figure 1b. In the proposed material, stimuli-responsive properties of the network and antifouling properties of the brush are decoupled. Thus, antifouling properties remain intact even if the material undergoes stimuli-triggered changes.

The 3D polymer-grafting can be carried out on the surface of polymers, nanofiber mats, and nanoporous inorganic materials, specifically in cases when hydrogel network coatings cannot be applied. The proposed self-healing system is a promising method for the end-grafted advanced polymer biointerfaces in biomedical and biotechnological applications.

4. Experimental Section

The cross-linked poly(2-vinyl pyridine) (P2VP, *Mn* = 152 kDa, Sigma-Aldrich) films on the surface of Si-wafers were prepared according to the previously-reported procedure.[53,54] 2 w/v% P2VP and 2 vol% diiodobutane (DIB, Sigma-Aldrich) were dissolved in a mixture of nitromethane and tetrahydrofuran (9:1volume ratio). The resulting solution was heated at 60–80 °C and stirred for different periods of time to approach a desired degree of quaternization. We previously reported that typically only one of two iodoalkyl groups in DIB reacted with P2VP pyridine rings in the reaction conditions. The solution was filtered and then spin-coated on the surface of silanized silicon wafers at 3000 rpm at a low humidity (<10 RH%). For samples with high quaternization degrees, prior to spin-coating, 0.5 vol% 4-propylphenol (Sigma-Aldrich) was added to the solution to prevent the phase separation of quaternized P2VP and DIB. The silanization of silicon wafers was carried out by immersing them overnight in a 1 wt% 11-bromoundecyldimethylchlorosilane (Gelest, Inc.) solution in dry toluene at RT. The obtained films were annealed at 100 °C in a vacuum for at least 1 h to complete the cross-linking reaction of P2VP with residual functional groups of DIB, and the immobilization reaction of the P2VP film via bromoalkyl groups on the silicon wafers. It was found that the thickness of the obtained P2VP films was ≈10–20 nm according to the ellipsometry measurements, and the water contact angle was about 70°. A Multiskop null-ellipsometer (Optrel) equipped with an He-Ne laser (λ = 633 nm) was used for ellipsometric measurements. The angle of incidence of polarized light was set at 70°. The surface of the prepared films was examined using atomic force microscopy (AFM, Dimension 3100 scanning probe microscope, Veeco Instruments). AFM images were processed using WSxM software.[59] The root mean square roughness for the samples was in the range from 0.2 to 0.5 nm.

PEO was next grafted to the surface and inside the P2VP network films. A 2 w/v% solution of halogen-terminated PEO in toluene was spin-coated on the P2VP network films at 3000 rpm, and the grafting reaction was conducted by annealing at 120 °C in a vacuum; the grafting temperature was higher than the glass transition temperature of P2VP and the melting temperature of PEO.[60,61] P2VP and PEO are miscible. Therefore, PEO chains can penetrate into the P2VP network, leading to the grafting of PEO to the surface and inside the P2VP film. After the grafting step, the films were rinsed with chloroform and an acidic aqueous solution (pH 2.0) for 1 day for each solvent to remove unreacted PEO, and then dried with a nitrogen gas flow. Three samples of halogen-terminated PEO were used; chloro-terminated PEO with *Mn* = 5.0 kDa (PEO-Cl-5k, Polymer Sources), bromo-terminated PEOs with *Mn* = 5.0 kDa (PEO-Br-5k) and *Mn* = 12.3 kDa (PEO-Br-12k). The bromo-terminated PEOs were synthesized according to the previously-reported procedure (see the Supporting Infromation for details).[62] The prepared PEO-grafted P2VP films were characterized using ellipsometry, X-ray reflectivity, water contact angle, and AFM measurements. Amount of the grafted PEO, Γ (mg/m^2), was calculated from the ellipsometric thickness, *h*, and the density (ρ = 1.09 g/cm^3) of PEO using the equation: $\Gamma = h\rho$.[55] X-ray reflectivity was measured in air with an Ultima III multipurpose diffractometer (Rigaku Corp.) in parallel beam geometry with a 100 mm vertical beam size and a Cu-tube as the X-ray source. Prior to the measurements, the prepared films were immersed in a tetrachloroauric acid aqueous solution at pH 2.0 for 1 h, and then washed with DI water. The tetrachloroauric ions were selectively bound to the P2VP layer in the films, and the scattering length density of the metal-bound P2VP layer is thus higher than that of the PEO layers. X-ray reflectivity measurements provide statistically averaged information over a large surface area (typically in the millimeter–centimeter range).

Antifouling properties of the PEO-grafted P2VP films were studied by protein adsorption tests using BSA (67 kDa, pI 4.7, Sigma-Aldrich) and fibrinogen (containing ≈15% sodium citrate and ≈25% sodium chloride, 340 kDa, pI 5.5, Sigma-Aldrich). A 1 mg/mL of protein solution in a phosphate buffer (pH 7.4) was deposited (as a thin liquid film) on the grafted surface and remained in contact with the coating at RT and high surrounding humidity for 1 h. Afterward, the films were rinsed with a phosphate buffer solution and distilled water, and then dried in a nitrogen gas flow. The adsorbed protein amount was evaluated using ellipsometry, and the adsorbed amount was calculated by multiplying the thickness of the adsorbed protein layer by its density.[40,63,64]

Supporting Information

Supporting Information is available from the Wiley Online Library or from the author.

Acknowledgements

This work was supported in part by Clarkson University and NSF award DMR 1107786. H.K. thanks the Japan Society for the Promotion of Science (JSPS, Japan) for the support of his research fellowship. Research carried out in part at the Center for Functional Nanomaterials, Brookhaven National Laboratory, which is supported by the U.S. Department of Energy, Office of Basic Energy Sciences, under Contract No. DE-AC02-98CH10886.

Received: January 30, 2013
Revised: April 19, 2013
Published online: June 3, 2013

[1] M. A. C. Stuart, W. T. S. Huck, J. Genzer, M. Mueller, C. Ober, M. Stamm, G. B. Sukhorukov, I. Szleifer, V. V. Tsukruk, M. Urban, F. Winnik, S. Zauscher, I. Luzinov, S. Minko, *Nat. Mater.* **2010**, *9*, 101.
[2] N. A. Peppas, J. Z. Hilt, A. Khademhosseini, R. Langer, *Adv. Mater.* **2006**, *18*, 1345.
[3] Z. Zhang, M. Zhang, S. F. Chen, T. A. Horbetta, B. D. Ratner, S. Y. Jiang, *Biomaterials* **2008**, *29*, 4285.
[4] I. Banerjee, R. C. Pangule, R. S. Kane, *Adv. Mater.* **2011**, *23*, 690.
[5] H. Kuroki, I. Tokarev, S. Minko, *Annu. Rev. Mater. Res.* **2012**, *42*, 343.
[6] K. Prime, G. Whitesides, *Science* **1991**, *252*, 1164.
[7] G. B. Sigal, M. Mrksich, G. M. Whitesides, *J. Am. Chem. Soc.* **1998**, *120*, 3464.
[8] M. H. Schoenfisch, J. E. Pemberton, *J. Am. Chem. Soc.* **1998**, *120*, 4502.
[9] Y. Y. Luk, M. Kato, M. Mrksich, *Langmuir* **2000**, *16*, 9604.
[10] V. A. Tegoulia, W. S. Rao, A. T. Kalambur, J. R. Rabolt, S. L. Cooper, *Langmuir* **2001**, *17*, 4396.
[11] S. F. Chen, J. Zheng, L. Y. Li, S. Y. Jiang, *J. Am. Chem. Soc.* **2005**, *127*, 14473.
[12] L. Y. Li, S. F. Chen, J. Zheng, B. D. Ratner, S. Y. Jiang, *J. Phys. Chem. B* **2005**, *109*, 2934.
[13] R. Chelmowski, S. D. Koster, A. Kerstan, A. Prekelt, C. Grunwald, T. Winkler, N. Metzler-Nolte, A. Terfort, C. Woll, *J. Am. Chem. Soc.* **2008**, *130*, 14952.
[14] T. Fyrner, H. H. Lee, A. Mangone, T. Ekblad, M. E. Pettitt, M. E. Callow, J. A. Callow, S. L. Conlan, R. Mutton, A. S. Clare, P. Konradsson, B. Liedberg, T. Ederth, *Langmuir* **2011**, *27*, 15034.
[15] T. Gillich, E. M. Benetti, E. Rakhmatullina, R. Konradi, W. Li, A. Zhang, A. D. Schluter, M. Textor, *J. Am. Chem. Soc.* **2011**, *133*, 10940.
[16] R. Barbey, L. Lavanant, D. Paripovic, N. Schuewer, C. Sugnaux, S. Tugulu, H.-A. Klok, *Chem. Rev.* **2009**, *109*, 5437.
[17] S. J. Sofia, V. Premnath, E. W. Merrill, *Macromolecules* **1998**, *31*, 5059.
[18] G. L. Kenausis, J. Voros, D. L. Elbert, N. P. Huang, R. Hofer, L. Ruiz-Taylor, M. Textor, J. A. Hubbell, N. D. Spencer, *J. Phys. Chem. B* **2000**, *104*, 3298.
[19] J. P. Bearinger, S. Terrettaz, R. Michel, N. Tirelli, H. Vogel, M. Textor, J. A. Hubbell, *Nat. Mater.* **2003**, *2*, 259.
[20] J. L. Dalsin, B. H. Hu, B. P. Lee, P. B. Messersmith, *J. Am. Chem. Soc.* **2003**, *125*, 4253.
[21] H. W. Ma, J. H. Hyun, P. Stiller, A. Chilkoti, *Adv. Mater.* **2004**, *16*, 338.
[22] S. Sharma, R. W. Johnson, T. A. Desai, *Langmuir* **2004**, *20*, 348.
[23] C. Siegers, M. Biesalski, R. Haag, *Chem. Eur. J.* **2004**, *10*, 2831.
[24] B. Zdyrko, S. K. Varshney, I. Luzinov, *Langmuir* **2004**, *20*, 6727.
[25] J. L. Dalsin, L. J. Lin, S. Tosatti, J. Voros, M. Textor, P. B. Messersmith, *Langmuir* **2005**, *21*, 640.
[26] O. Hoy, B. Zdyrko, R. Lupitskyy, R. Sheparovych, D. Aulich, J. F. Wang, E. Bittrich, K. J. Eichhorn, P. Uhlmann, K. Hinrichs, M. Muller, M. Stamm, S. Minko, I. Luzinov, *Adv. Funct. Mater.* **2010**, *20*, 2240.
[27] D. W. Branch, B. C. Wheeler, G. J. Brewer, D. E. Leckband, *Biomaterials* **2001**, *22*, 1035.
[28] X. W. Fan, L. J. Lin, P. B. Messersmith, *Biomacromolecules* **2006**, *7*, 2443.
[29] J. E. Raynor, T. A. Petrie, A. J. Garcia, D. M. Collard, *Adv. Mater.* **2007**, *19*, 1724.
[30] S. Tugulu, H. A. Klok, *Biomacromolecules* **2008**, *9*, 906.
[31] V. Zoulalian, S. Zurcher, S. Tosatti, M. Textor, S. Monge, J. J. Robin, *Langmuir* **2010**, *26*, 74.
[32] C. Yoshikawa, A. Goto, Y. Tsujii, T. Fukuda, T. Kimura, K. Yamamoto, A. Kishida, *Macromolecules* **2006**, *39*, 2284.
[33] C. Zhao, L. Y. Li, Q. M. Wang, Q. M. Yu, J. Zheng, *Langmuir* **2011**, *27*, 4906.
[34] N. B. Holland, Y. X. Qiu, M. Ruegsegger, R. E. Marchant, *Nature* **1998**, *392*, 799.
[35] M. Metzke, J. Z. Bai, Z. B. Guan, *J. Am. Chem. Soc.* **2003**, *125*, 7760.
[36] C. Perrino, S. Lee, S. W. Choi, A. Maruyama, N. D. Spencer, *Langmuir* **2008**, *24*, 8850.
[37] W. Feng, S. P. Zhu, K. Ishihara, J. L. Brash, *Langmuir* **2005**, *21*, 5980.
[38] S. Y. Jiang, Z. Q. Cao, *Adv. Mater.* **2010**, *22*, 920.
[39] A. T. Nguyen, J. Baggerman, J. M. J. Paulusse, C. J. M. van Rijn, H. Zuilhof, *Langmuir* **2011**, *27*, 2587.
[40] S. Colak, G. N. Tew, *Langmuir* **2012**, *28*, 666.
[41] R. Konradi, B. Pidhatika, A. Muhlebach, M. Textort, *Langmuir* **2008**, *24*, 613.
[42] A. R. Statz, A. E. Barron, P. B. Messersmith, *Soft Matter* **2008**, *4*, 131.
[43] S. H. Lin, B. Zhang, M. J. Skoumal, B. Ramunno, X. P. Li, C. Wesdemiotis, L. Y. Liu, L. Jia, *Biomacromolecules* **2011**, *12*, 2573.
[44] A. Worz, B. Berchtold, K. Moosmann, O. Prucker, J. Ruhe, *J. Mater. Chem.* **2012**, *22*, 19547.
[45] R. Yoshida, K. Uchida, Y. Kaneko, K. Sakai, A. Kikuchi, Y. Sakurai, T. Okano, *Nature* **1995**, *374*, 240.
[46] H. K. Ju, S. Y. Kim, Y. M. Lee, *Polymer* **2001**, *42*, 6851.
[47] Z. L. Tang, Y. Akiyama, M. Yamato, T. Okano, *Biomaterials* **2010**, *31*, 7435.
[48] T. Inoue, G. H. Chen, K. Nakamae, A. S. Hoffman, *J. Controlled Release* **1997**, *49*, 167.
[49] S. Asayama, M. Nogawa, Y. Takei, T. Akaike, A. Maruyama, *Bioconjugate Chem.* **1998**, *9*, 476.

[50] F. J. Xu, Y. Ping, J. Ma, G. P. Tang, W. T. Yang, J. Li, E. T. Kang, K. G. Neoh, *Bioconjugate Chem.* **2009**, *20*, 1449.
[51] F. J. Xu, Y. Zhu, F. S. Liu, J. Nie, J. Ma, W. T. Yang, *Bioconjugate Chem.* **2010**, *21*, 456.
[52] S. Samanta, D. P. Chatterjee, S. Manna, A. Mandal, A. Garai, A. K. Nandi, *Macromolecules* **2009**, *42*, 3112.
[53] I. Tokarev, M. Orlov, S. Minko, *Adv. Mater.* **2006**, *18*, 2458.
[54] M. Orlov, I. Tokarev, A. Scholl, A. Doran, S. Minko, *Macromolecules* **2007**, *40*, 2086.
[55] B. Zdyrko, V. Klep, I. Luzinov, *Langmuir* **2003**, *19*, 10179.
[56] B. Wieland, J. P. Lancaster, C. S. Hoaglund, P. Holota, W. J. Tornquist, *Langmuir* **1996**, *12*, 2594.
[57] S. Han, C. Kim, D. Kwon, *Polymer* **1997**, *38*, 317.
[58] A. Halperin, M. Kroeger, E. B. Zhulina, *Macromolecules* **2011**, *44*, 3622.
[59] I. Horcas, R. Fernandez, J. M. Gomez-Rodriguez, J. Colchero, J. Gomez-Herrero, A. M. Baro, *Rev. Sci. Instrum.* **2007**, *78*, 8.
[60] K. Pielichowski, K. Flejtuch, *Polym. Adv. Technol.* **2002**, *13*, 690.
[61] P. Papadopoulos, D. Peristeraki, G. Floudas, G. Koutalas, N. Hadjichristidis, *Macromolecules* **2004**, *37*, 8116.
[62] J. L. Vanderhooft, B. K. Mann, G. D. Prestwich, *Biomacromolecules* **2007**, *8*, 2883.
[63] P. Cuypers, J. Corsel, M. Janssen, J. Kop, W. Hermens, H. Hemke, *J. Biol. Chem.* **1983**, *258*, 2426.
[64] H. Elwing, *Biomaterials* **1998**, *19*, 397.